ISSN: 2633-4828 Vol. 5 No.4, December, 2023

International Journal of Applied Engineering and Technology

Lung Image Generation based on Layered Two-Stages Generative Adversarial Networks

Wanle Chi[1]

[1]*Wenzhou Cyber Security Detection and Protection Technology Research Center, Wenzhou Polytechnic, China*
Faculty of Information and Communication Technology, Universiti Teknikal Malaysia Melaka, Malaysia
College of artificial intelligence, Wenzhou Polytechnic, China, e-mail:chiokchi@163.com

Yunhuoy Choo[2], Yogan Jaya Kumar[3]

[2,3]*Faculty of Information and Communication Technology, Universiti Teknikal Malaysia Melaka, Malaysia,*
e-mail:huoy@utem.edu.my, yogan@utem.edu.my

Shunda Cai[4]

[4]*College of artificial intelligence, Wenzhou Polytechnic, China,* e-mail:askatsoi@163.com

Date of Submission: 21st October 2023 Revised: 12th November 2023 Accepted: 24th November 2023

How to Cite: **Wanle Chi, Yunhuoy Choo, Yogan Jaya Kumar and Shunda Cai(2023). Lung Image Generation based on Layered Two-Stages Generative Adversarial Networks. International Journal of Applied Engineering Research 5(1), pp.121-127.**

Abstract **-The acquisition of large datasets poses a challenge due to issues related to privacy and radiation. In the case of medical image datasets, they are highly unbalanced, primarily consisting of healthy tissue data, while unhealthy data requires classification into different categories. Furthermore, the volume of data varies significantly between these categories. To enhance the accuracy of deep learning algorithms for medical assisted diagnosis, it is crucial to address the datasets imbalance problem.**

This paper proposes a method to extend the medical image datasets by utilizing layered two-stages Generative Adversarial Networks. The first stage of this approach involves a two-layer GAN generator. The first layer generates lung nodules, while the second layer generates normal lung images. These generated lung nodules are then overlaid on the normal images to produce the desired lung images, significantly enhancing the diversity of the outputs. The second stage involves utilizing Cycle GAN to improve the .exhibits superior data expansion capability compared to other methods and enhances the quality of synthetic images.

keywords **- Lung ; Image Generation; Two-Stages; Cycle GAN; CapsuleGAN.**

INTRODUCTION

The application of deep learning algorithms in medical imaging has garnered significant attention, effectively bridging the realms of medicine and computing.

In the context of computer-aided diagnosis, the quantity and diversity of the required datasets play a crucial role in shaping the final training effect of deep learning models. However, concerns around privacy and the harmful effects of radiation exposure pose substantial challenges to researchers in acquiring a large quantity of medical image datasets. Furthermore, healthy data often dominate such datasets, leading to slow convergence or overfitting of the model[1][2][3].

This substantial imbalance in the dataset can significantly impact the accuracy of deep learning algorithms utilized in medical assisted diagnosis. Addressing this issue of datasets imbalance is thus essential to enhance the performance of deep learning algorithms for medical assistance diagnosis[4][5].

Therefore, the expansion of medical image datasets in simulated images using artificial intelligence has emerged as a pressing issue in the domain of computer-aided diagnosis. One potential solution to this challenge is the generative adversarial network (GAN) conceptualized by Goodfellow et al. GANs, along with their variants, have gained widespread acceptance in medical image synthesis due to their diverse advantages[6,7].

The paper presents a novel approach for synthesizing lung images using a layered two-stages generative adversarial network.

The primary objective of this method is to balance the data volume across various lung diseases, thereby enhancing the accuracy of computer-aided medical diagnosis methods.

DATASETS AND PREPROCESSION

I. Nodule Extraction

The datasets used in this study are from The First Affiliated Hospital of Wenzhou Medical University, which comprise over 1,000 CT lung images. The labeled datasets encompass participant characteristics, exam results, diagnostic procedures, and mortality information.

Notably, the datasets does not provide coordinates of nodules within the CT images.

To address this limitation, the paper proposes an enhanced U-Net architecture to extract nodules from CT images. This enhancement allows for the consideration of images without nodules as normal images, thereby balancing the data volume across various lung diseases.

To mitigate overfitting, a batch normalization module is incorporated into the network encoder. This modification to the improved U-Net design proposes the addition of denseNet blocks to the network decoder to enhance feature reuse[8,9]. The combination of denseNet+U-Net architecture offers a compact structure that maximizes information flow between layers, thereby reducing vanishing gradient and overfitting. The denseNet block's structure is illustrated in Figure 1 of the paper.

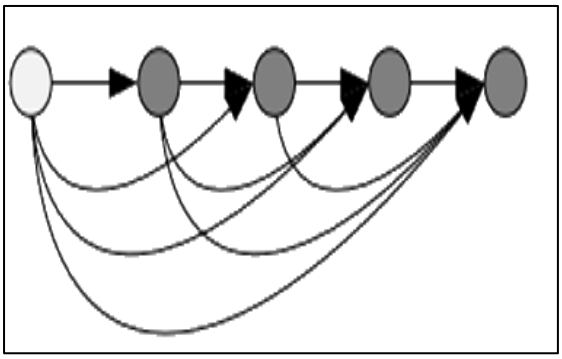

FIGURE 1 THE STRUCTURE OF DENSENET BLOCK.

The first layer of the dense block takes the feature diagrams of all previous layers as input, which shows in formula 1.

$$x_l = H_l([x_0, x_1, \ldots, x_{l-1}]) \qquad (1)$$

$H_l(.)$represents nonlinear transformation operations such as convolution.

To address the differences in the sizes of the shallow and deep layers during upsampling, transposed convolution is employed. This adaptation allows the model to better fit the deep layers, enhancing its performance. The improved U-Net architecture, along with its structure, is illustrated in Figure 2 of the paper.

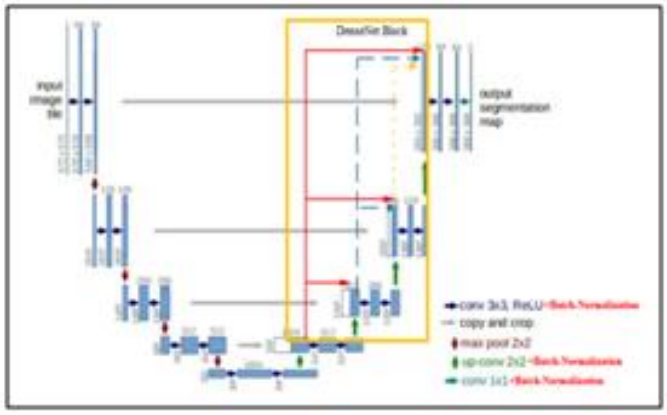

FIGURE 2 THE STRUCTURE OF IMPROVED U-NET.

The CT datasets are separated into nodule datasets and normal datasets, see Figure 3.

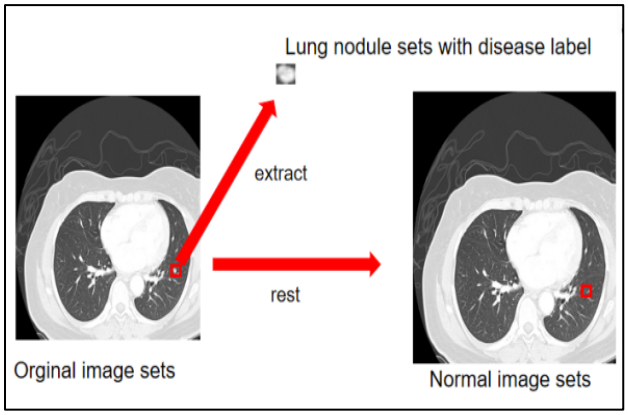

FIGURE 3 THE NODULES & NORMAL IMAGES.

To assess the effectiveness of this method, the paper presents its evaluation on the LUNA16 datasets. The LUNA16 datasets is a subset of the publicly available lung nodule datasets, LIDC-IDRI (Lung Image Database Consortium-Image Database Resource Initiative). Each image in the datasets contains nodule coordinates obtained from four radiologists, as illustrated in Figure 4 of the paper.

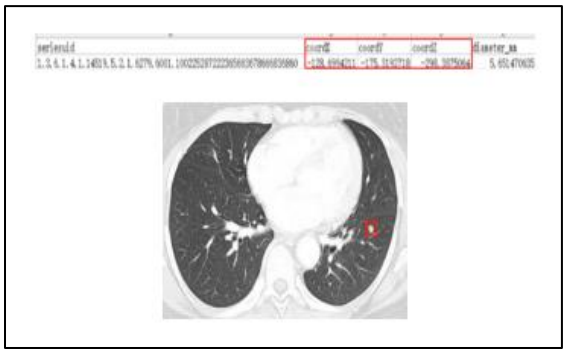

FIGURE4 THE NODULE COORDINATES FROM FOUR RADIOLOGISTS.

TABLE I
THE COMPARISON OF SEGMENTATION OF DIFFERENT METHODS.

Method	Sensitivity	Number of segmented nodules	Accuracy
CNN+VGG	91.32%		92.64%
Faster RCNN +3DDCNN	93.54%	15.0	
U-Net	93.2%	8.0	87.3%
U-Net++	89.7%	32.5	
This method	94.3%	12.2	96.3%

The method proposed in this paper outperforms other algorithms in terms of accuracy when evaluated on the same LUNA16 datasets. While the speed of the method is relatively slower compared to U-Net, it addresses the missing feature detection issue by reusing features in the dense block, resulting in improved recognition accuracy.

The CNN+VGG model has a deeper network depth but lacks network structure tricks, which leads to lower accuracy than the proposed method[10]. Additionally, the sensitivity of the method proposed in this paper is higher than other algorithms. While the number of candidate nodules detected by U-Net is lower than that of the algorithm proposed in this paper, our method exhibits both high sensitivity and accuracy.

II. Image Generator of Based on W-CapsuleGAN

The lung nodule images in the study were in low-resolution grayscale format, which limited the performance of the GAN model used for generating variations. The nodule data resembled black-and-white handwriting images compared to color images like CIFAR-10, and as such, color image generators such as BigGAN, which performed well on color images, did not fare well on the low-resolution gray nodule images[11].

This issue could have been due to mode collapse in GANs or an inappropriate loss function being selected. The hinge loss function may not have been suitable for the nodule generator. Algorithms such as DCGAN, Wasserstein-GAN, and CapsuleNets were more suitable for tasks involving handwriting recognition[12,13,14].

To overcome the low classification performance on nodule datasets, this paper proposed a W-CapsuleGAN model. The model used CapsuleNets instead of a deep convolutional network and employed the wasserstein distance as the loss function.

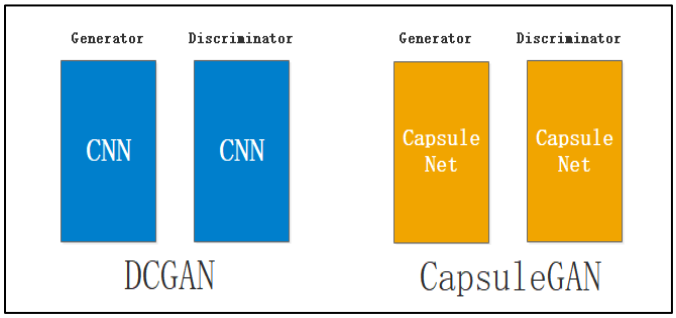

FIGURE 5 THE STRUCTURE OF CAPSULEGAN.

The loss function used by the original Capsule GAN is margin. The principle of margin function is similar to the Hinge loss function of BigGAN, which may not be suitable for gray images. In this case, the paper proposes using the Wasserstein distance as the loss function.

The Wasserstein distance is a measure of the Earth Mover's distance between two probability distributions. It is defined as follows:

$$W(P_r, P_g) = inf_{\gamma=\prod(P_r,P_g)} E_{(x,y)\sim\gamma}[||x-y||] \quad (2)$$

The experiment was conducted by dividing the nodule datasets into a training set and a testing set following a 4:1 ratio. This means that 40% of the data was used for training the model, while the remaining 60% was used for testing the model's performance.The nodule generation process was executed using a method that involved supplementation of 200 examples in each category. This means that for each category, 200 additional examples were added to the training set to increase the diversity of the datasets and improve the model's ability to generalize to new examples.

TABLE II
THE EXPERIMENTAL RESULT OF W-CAPSULEGAN.

Method	IS(Inception Score)	FID(Fréchet Inception Distance)
BigGAN	1.6	233
GAN	5.4	74.2
DCGAN	5.9	84.3
WGAN	7.2	54.5
CapsuleNets	7.5	102.1
W-CapsuleGAN	7.9	30.2

LAYERED TWO-STAGES GENERATIVE ADVERSARIAL NETWORKS

Direct generation of highly similar lung images is primarily due to common features and structures shared by these images. Lung images from various modalities display basic features like pulmonary parenchyma, bronchi, blood vessels, and heart structures, which contribute to direct images' high similarity. However, practical difficulties in controlling these factors result in high similarity of directly generated lung images. Furthermore, the diversity and similarity of GANs are also influenced by training data quantity and diversity. A small/diverse datasets results in high similarity, while a large and diverse datasets increases diversity. GANs may learn pulmonary structures and lesion characteristics with sufficient diverse datasets and generate more diverse lung images. However, due to original sample scarcity, direct generation of lung images often results in high similarity and insufficient diversity[15,16,17].

The generator of lung images typically struggles to strike a balance between diversity and similarity. This paper proposes a layered two-stages GAN algorithm to address both issues. The first stage of the algorithm is to train a two layers generator to generate more diverse images, while the second stage is to train a Cycle GAN enhanced generator to improve image similarity. In the first stage, the proposed GAN algorithm uses a single generator network that is trained to generate diverse lung images. By training the generator to generate a diverse set of images, the algorithm can produce a wide range of variations in terms of appearance and structure.

In the second stage, the proposed algorithm uses a Cycle GAN enhanced generator network to improve the similarity of the generated lung images. The Cycle GAN enhances the generator by adding an additional discriminator network that evaluates the realism of the generated images. This additional discriminator network helps to ensure that the generated images are not only diverse but also realistic and similar to real lung nodules. By combining the outputs of the two generator networks in the second stage, the proposed Two-Stages GAN algorithm produces lung images that are both diverse and similar to real lung nodules.

This approach can help overcome the limitations of traditional GAN models and produce high-quality lung image datasets that are suitable for various applications such as medical diagnosis, drug development, and research[18].

I. Two Layers GAN Generator

The first stage is a two layers GAN generator, layer I generates lung nodules, and layer II generate normal lung images, overlays the generated lung nodules on the normal image to generate the specified lung image. This approach can significantly increase the diversity of generated outputs.

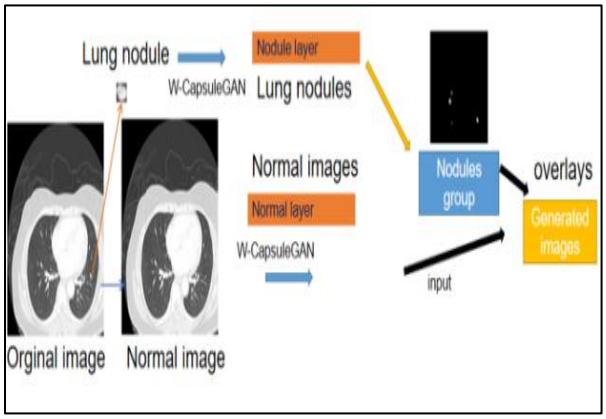

FIGURE 6 THE FIRST STAGE: TWO LAYERS GAN GENERATOR FOR LUNG IMAGES.

This study segmented images into nodules and normal regions, generating independent datasets. The datasets were created based on the morphology of lung parenchyma and the probability of nodule presence, creating a nodule-randomized group datasets. Generated nodules groups and generated normal images were combined into new synthetic lung images and fed into the Cycle GAN.

50 images were randomly selected for each medical condition, from which 100-300 valid nodules were extracted, and generated 1000 nodules with the highest similarity were selected. In each disease, 200 real nodules were randomly selected and mixed with 1000 generated nodules, based on the probability of nodule presence, to generate 5000 of nodules groups. Similarly, for each disease, 50 normal lung images were selected after partitioning. W-CapsuleGAN was used to generate 450 synthetic normal images with the highest similarity, which were mixed real 50 normal lung images together to form 500 normal lung images.

Diseased lung images were generated by overlaying nodule groups onto normal lung images. The total number of generated images was 2,500,000 (500 * 5000 = 2,500,000).1,000,000 synthetic images that were farthest from the edge of the lung parenchyma were selected as the final output, successfully achieving a nearly 100,000-fold increase in generation volume. Other methods for lung image synthesis typically achieve a maximum multiplication factor of less than 1000.

This method greatly expands the diversity of medical image synthesis. The methodology proposed in the paper is suitable for the synthesis and enhancement of medical datasets with minimal raw data.

II. Cycle GAN Enhancer

The use of a two layers GAN generator may inevitably lead to poor quality of the synthesized images. Next, the second stage is to use Cycle GAN to enhance the similarity of the synthesized images.

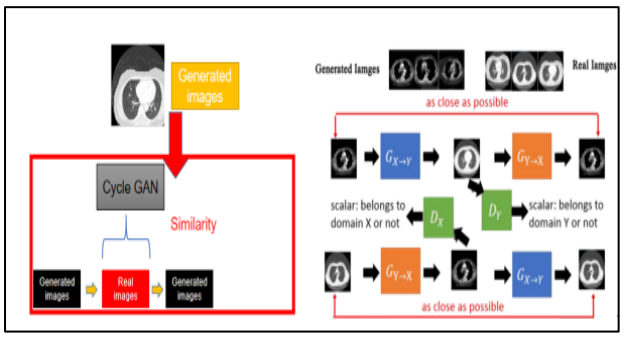

FIGURE 7 THE SECOND STAGE:CYCLE GAN ENHANCED GENERATOR.

To prevent impacting on the diversity of images, excluding images used for generation, another 100 images were randomly selected by this paper. And, 1,000,000 synthetic images were generated as the image set. The experiment demonstrates that cycle GAN enhanced synthetic images significantly enhance the quality of image generation while maintaining diversity.

TABLE III
THE EXPERIMENTAL RESULT OF TWO-STAGES GAN.

Method	IS(Inception Score)	FID(Fréchet Inception Distance)
BigGAN	1.3	418
GAN	4.7	202.9
DCGAN	6.9	184.1
WGAN	5.2	147.7
Two-Stages GAN	12.1	2.6

CONCLUSION

The Layered Two-Stages Generative Adversarial Networks proposed in this paper not only improve the quality of medical image synthesis but also greatly enhance diversity. The main contribution of the paper lies in proposing a Two-Stages approach that remedies the deficiency of other methods by separately addressing the diversity and similarity. The two layers GAN generator can significantly expand the number of generated images; the second stage enhances the generated results after screening and can effectively improve image quality. This method is particularly suitable for image datasets with few original samples. Experimental results indicate that the method proposed in this paper exhibits better data expansion capabilities and enhances the quality of synthetic images compared to other methods.

ACKNOWLEDGMENTS

This work was supported by the School-Enterprise Cooperation Project of Visiting Engineer of Education Department of Zhejiang Province (NO.FG2022056) and the Scientific Research Project of Zhejiang Natural Science Foundation, P.R. China (No.LY20G030018).

REFERENCES

[1] Chawla N,Bowyer K,O. Hall L,et al. Smote: Synthetic minority oversampling technique [J], Journal of Artificial Intelligence Research (JAIR), 2012,16: 321-357.

[2] Dalmaz O. Novel deep learning algorithms for multi-modal medical image synthesis[D]. bilkent university, 2023.

[3] Singh S, Ranapurwala A, Bewoor M, et al. Systematic Review of Techniques in Brain Image Synthesis using Deep Learning[J]. arXiv preprint arXiv:2309.04511, 2023.

[4] Armato Iii S, Mclennan G, Bidaut L, et ai. The lung image database consortium (lidc) and image database resource initiative (idri): A completed reference database of lung nodules on ct scans [J]. Medical Physics, 2021,38: 915-931.

[5] Mcnitt-Gray M F,Armato S G,Meyer C et al. The lung image database consortium (lidc) data collection process for nodule detection and annotation [J]. Academic Radiology, 2017, 14(12): 1464-1474.

[6] Nie D, Trullo R, Lian J, et al. Medical image synthesis with deep convolutional adversarial networks [J]. IEEE Transactions on Biomedical Engineering, 2019,65(12): 2720-2730.

[7] Frid-Adar M, Klang E, Amitai M, et al. Synthetic data augmentation using gan for improved liver lesion classification [C] //IEEE 15th International Symposium on Biomedical Imaging(ISBI). 2021: 289-293.

[8] Huang G, Liu Z, Van Der Maaten L, et al. Densely connected convolutional networks[C]//Proceedings of the IEEE conference on computer vision and pattern recognition. 2017: 4700-4708.

[9] Ronneberger O, Fischer P, Brox T. U-net: Convolutional networks for biomedical image segmentation[C]//Medical Image Computing and Computer-Assisted Intervention–MICCAI 2015: 18th International Conference, Munich, Germany, October 5-9, 2015, Proceedings, Part III 18. Springer International Publishing, 2015: 234-241.

[10] Simonyan K, Zisserman A. Very deep convolutional networks for large-scale image recognition[J]. arXiv preprint arXiv:1409.1556, 2014.

[11] Brock A, Donahue J, Simonyan K. Large scale GAN training for high fidelity natural image synthesis[J]. arXv preprint arXiv:1809.11096, 2018.

[12] Radford A, Metz L, Chintala S. Unsupervised representation learning with deep convolutional generative adversarial networks[J]. arXiv preprint arXiv:1511.06434, 2015.

[13] Arjovsky M, Chintala S, Bottou L. Wasserstein generative adversarial networks[C]//International conference on machine learning. PMLR, 2017: 214-223..

[14] Sabour S, Frosst N, Hinton G E. Dynamic routing between capsules[J]. Advances in neural information processing systems, 2017, 30.

[15] Han Y, Chen C, Tewfik A, et al. Pneumonia detection on chest x-ray using radiomic features and contrastive learning[C]//2021 IEEE 18th International Symposium on Biomedical Imaging (ISBI). IEEE, 2021: 247-251.

[16] Touloumes N, Kalra A, Bradley J A, Et Al. Artificial Intelligence In Incidental Detection Of Lung Fibrosis By Computed Tomography[J]. Chest, 2023, 164(4): A3085-A3086.

[17] Choi C, Thor M, Jiang J, et al. Determining the Dosimetric Accuracy of Deep Learning-Based Fully Automated Registration-Segmentation Approach for Thoracic Cancer Organs-at-Risk Contouring[J]. International Journal of Radiation Oncology, Biology, Physics, 2023, 117(2): e656-e657.

[18] Zhu J Y, Park T, Isola P, et al. Unpaired image-to-image translation using cycle-consistent adversarial networks[C]//Proceedings of the IEEE international conference on computer vision. 2017: 2223-2232.

AUTHOR INFORMATION

WanleChi, Vice Professor, College of Artificial Intelligence, Wenzhou Polytechnic.

YunHuoy Choo, Associate Professor and PhD Supervisor**,** Technical University of Malaysia Malacca.

Yogan JayaKumar, Associate Professor and PhD Supervisor**,** Technical University of Malaysia Malacca.

Shunda Cai, Engineer and Lecturer, College of Artificial Intelligence, Wenzhou Polytechnic.